

MOLECULAR GAS BAR AND EXPANDING MOLECULAR RING IN THE NUCLEUS OF THE SPIRAL GALAXY MAFFEI 2

M. ISHIGURO,¹ R. KAWABE,¹ K.-I. MORITA,¹ S. K. OKUMURA,² Y. CHIKADA,¹ T. KASUGA,¹ T. KANZAWA,¹
 H. IWASHITA,¹ K. HANDA,¹ T. TAKAHASHI,¹ H. KOBAYASHI,¹ Y. MURATA,² S. ISHIZUKI,² AND N. NAKAI¹

Received 1988 October 24; accepted 1989 March 2

ABSTRACT

Aperture synthesis observations of the central 1.5 kpc region of the spiral galaxy Maffei 2 ($d \sim 5$ Mpc) have been made in CO($J = 1-0$) line with $5''.8 \times 5''.0$ resolution (~ 135 pc) using the Nobeyama Millimeter Array. We have found a central narrow ridge of molecular gas with a size $1000 \text{ pc} \times 200 \text{ pc}$ and a ringlike feature with a large noncircular motion (60 km s^{-1}) with a size $500 \text{ pc} \times 240 \text{ pc}$. The narrow ridge is interpreted as a bar of molecular gas in shocks generated at the leading edges in the bar potential. The molecular bar has a mass of $(1-5) \times 10^8 M_{\odot}$, and there is a depression in the molecular gas distribution within 100 pc of the nucleus. The observational results suggest that the ring is an expanding and rotating ring of molecular gas in the plane of the galaxy, $V_{\text{exp}} \sim 60 \text{ km s}^{-1}$ and $M_{\text{ring}} \sim (3-13) \times 10^7 M_{\odot}$. The kinetic energy of expansion is $>(1-5) \times 10^{54}$ ergs and a dynamical expansion time scale is $\sim 5 \times 10^6$ yr (resultant kinetic luminosity is $[1-8] \times 10^6 L_{\odot}$). This energy and luminosity require an explosive event at the nucleus. The ring may have been formed by a starburst induced by the efficient gas supply in the bar potential.

Subject headings: galaxies: individual (Maffei 2) — galaxies: internal motions — galaxies: interstellar matter — galaxies: nuclei — galaxies: structure — interferometry

I. INTRODUCTION

Maffei 2 is a heavily obscured infrared object toward the plane of our Galaxy, first noted by Maffei (1968) and identified as a nearby spiral galaxy ($d \sim 5$ Mpc) by Spinrad *et al.* (1971, 1973). The morphological type is Sbc according to observations at optical, infrared, and radio wavelengths (Allen and Raimond 1972; Spinrad *et al.* 1973; Love 1972). It has been difficult to study the structure and kinematics because Maffei 2 is located at low Galactic latitude, $b \sim -0.5$ and has an LSR velocity near 0 km s^{-1} ; observations in H I and even in the infrared were severely affected by confusion due to foreground emission in our Galaxy (Bottinelli *et al.* 1971; Love 1972; Wright and Seielstad 1973). The detection of CO($J = 1-0$) emission (Rickard, Turner, and Palmer 1977), however, made it possible to determine the inner structure without severe confusion. CO($J = 2-1$) observations ($30''$ resolution) by Sargent *et al.* (1985) have revealed that CO emission is confined to the central 740 pc ($30''$) region. CO($J = 1-0$) mapping with $23''$ resolution by Weliachew, Casoli, and Combes (1988) found elongated CO emission along the major axis of the galaxy and a velocity field suggesting oval distortion of the gravitational potential. There is rather strong nonthermal radio emission from the disk similar to the late-type spirals NGC 6946 and M51 (Allen and Raimond 1972; Seaquist, Pfund, and Bignell 1976) and a (nonthermal) continuum source at the nucleus 100 times stronger than Sgr A (Seaquist, Pfund, and Bignell 1976).

In this paper, we present $5''.8 \times 5''.0$ resolution CO($J = 1-0$) maps in the central 1.5 kpc region of Maffei 2. The maps show a narrow molecular bar and a ring with large noncircular motion explained as expansion. We will discuss the molecular bar and the ring with its origin of expansion.

II. OBSERVATIONS

The central region of Maffei 2 was observed in $J = 1-0$ line of CO with the Nobeyama Millimeter Array (Ishiguro *et al.* 1984, 1989) on 1988 May 6 and 9. The array consists of five 10 m antennas which are equipped with new SIS receivers (Kawabe *et al.* 1989) developed at the Nobeyama Radio Observatory (NRO). Their system noise temperatures (SSB) were 600–700 K at the zenith. We used an FFT spectroc correlator with 1024 channels per baseline, called an FX (Chikada *et al.* 1987). The bandwidth of the observations was 320 MHz, which covered a velocity of 830.8 km s^{-1} at 115 GHz, and the velocity resolution was 0.81 km s^{-1} .

A 10 minute observation of 3C 84 was taken every 30 minutes in order to calibrate the gain and phase of the array. The bandpass across the 1024 frequency channels was determined from the 30 minute observation of 3C 84 with an accuracy of 6% rms in amplitude and 5° rms in phase. Flux density of 3C 84 was determined from the observations of Uranus. We assumed the brightness temperature of Uranus is 120 K at 115 GHz based on the measurements by Ulich (1981; 3.3 mm) and Gear *et al.* (1985; 0.4–2.0 mm) and the flux density of 3C 84 was estimated to be $18.4 \pm 2 \text{ Jy}$.

After these calibrations, the maps were made and CLEANed in the conventional manner using the NRAO AIPS package. We used the same array configuration with baselines from 20 m to 70 m for two observations and the duration of each observation was 8 hr. The synthesized beam was $5''.8 \times 5''.0$ (FWHM) with its major axis in position angle of -29° . The rms noise level of the maps with a velocity width of 9.75 km s^{-1} was about $0.18 \text{ Jy beam}^{-1}$. The maps were not corrected for the primary beam of the 10 m antenna. Observational parameters are summarized in Table 1.

III. RESULTS

Figure 1a shows a map of the CO($J = 1-0$) intensity integrated over a velocity range 234.0 km s^{-1} wide from $V_{\text{lsr}} = -156.2 \text{ km s}^{-1}$ to 77.8 km s^{-1} . A contour interval is 60 K km

¹ Nobeyama Radio Observatory, National Astronomical Observatory. Nobeyama Radio Observatory is a branch of the National Astronomical Observatory, the Ministry of Education, Science, and Culture of Japan.

² Department of Astronomy, University of Tokyo.

TABLE 1
OBSERVATIONAL PARAMETERS

Parameter	Value
Telescope	Nobeyama Millimeter Array
Date	1988 May 6 and 9
Source	Maffei 2
Field center	R.A. (1950) = $2^{\text{h}}38^{\text{m}}8^{\text{s}}.492$; Decl. (1950) = $59^{\circ}23'24''0$
Field of view	$65''$
Longest baseline	$27 \text{ k}\lambda$
Shortest baseline	$7 \text{ k}\lambda$
Synthesized beam	$5''.8 \times 5''.0$ (at P.A. -29°)
Center frequency	115.21 GHz
Total bandwidth	320 MHz
Velocity resolution	0.81 km s^{-1}
Visibility and bandpass calibrator	3C 84 (18.4 Jy)
Flux calibrator	Uranus ($T_b = 120 \text{ K}$)

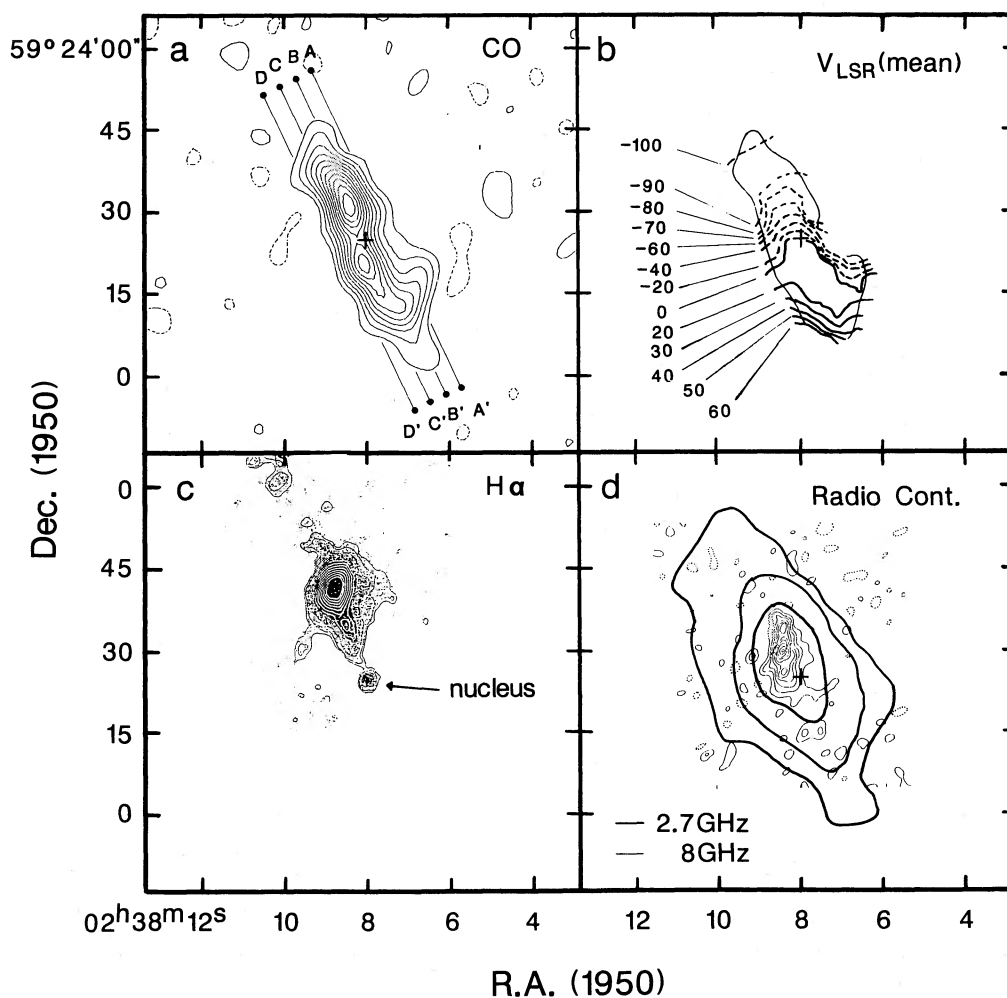


FIG. 1.—(a) A map of CO intensity ($\int T_B dv$) integrated over 234.0 km s^{-1} , from $V_{\text{lsr}} = -156.2 \text{ km s}^{-1}$ to 77.8 km s^{-1} . A contour interval is 60 K km s^{-1} (2σ noise level of the map). (b) A CO velocity field in which velocities are weighted by intensities calculated using channel maps (see Fig. 2). (c) A map of H α emission (Spinrad and McCarthy 1988). (d) Maps of radio continuum emissions at 2.7 and 8 GHz (Seaquist *et al.* 1976). A cross indicates a position of the nuclear H α peak, R.A. (1950) = $02^{\text{h}}38^{\text{m}}7^{\text{s}}.98$, decl. (1950) = $59^{\circ}23'24''.9$.

s^{-1} which corresponds to 2σ noise level of the map. The total flux in the map is $1460 \pm 200 \text{ Jy km s}^{-1}$. Total single-dish flux of $\text{CO}(J=1-0)$ is $2440 \text{ Jy km s}^{-1}$. It is estimated from the observations by the $56''$ beam of the OVRO 10.3 m telescope (Sargent *et al.* 1985) and includes weak emission ($0.1\text{--}0.2 \text{ K}$) over 430 km s^{-1} . The total flux in the same velocity range as that of our CO map is roughly 1900 Jy . Our integrated flux is, therefore, $60\% \pm 10\%$ of the total single-dish flux and our interferometer map samples more than $80\% \pm 10\%$ of the single dish flux at the same velocity range, 234 km s^{-1} .

The map shows a very narrow ridge with a position angle (P.A.) of $25^\circ\text{--}30^\circ$ roughly aligned along the major axis of the galaxy (P.A. = 30°). The ridge extends to $43''$ (1050 pc) \times $9''$ (220 pc) at the 4σ contour level and the size at the half-intensity is $30''$ (740 pc) \times $7''$ (160 pc). The deconvolved size along the minor axis of the ridge is about $4''$ (100 pc). In addition to the narrow ridge structure, the following interesting structures can be seen. (1) The narrow ridge has two peaks at

opposite sides of the southern nuclear $\text{H}\alpha$ peak (Spinrad and McCarthy 1988), R.A. (1950.0) = $02^{\text{h}}38^{\text{m}}7^{\text{s}}.98$, decl. (1950.0) = $59^\circ23'24''.9$. Hereafter, we refer this position as the nucleus of Maffei 2. (2) The northern and southern halves of the ridge are misaligned (see Fig. 4b); the shift of the ridge line is about $3''\text{--}4''$. (3) There is an arclike feature at the southern end of the ridge.

A ratio of the major axis to the minor axis in the narrow ridge is greater than 5. A disk would have the ratio of about 2 assuming the same inclination angle as the galaxy, $i = 55^\circ\text{--}70^\circ$ (Bottinelli 1981; Love 1972; Allen and Raimond 1972; Shostak and Weliachew 1971; Wright and Seielstad 1973). The molecular ridge, therefore, cannot be explained as a disk of molecular gas. Another interpretation is that the ridge is a bar of molecular gas (see § IVa).

Figure 1b shows a map of CO isovelocity contours made using mean velocities weighted by CO intensities from channel maps (Fig. 2). The velocity structure is not easy to interpret. In

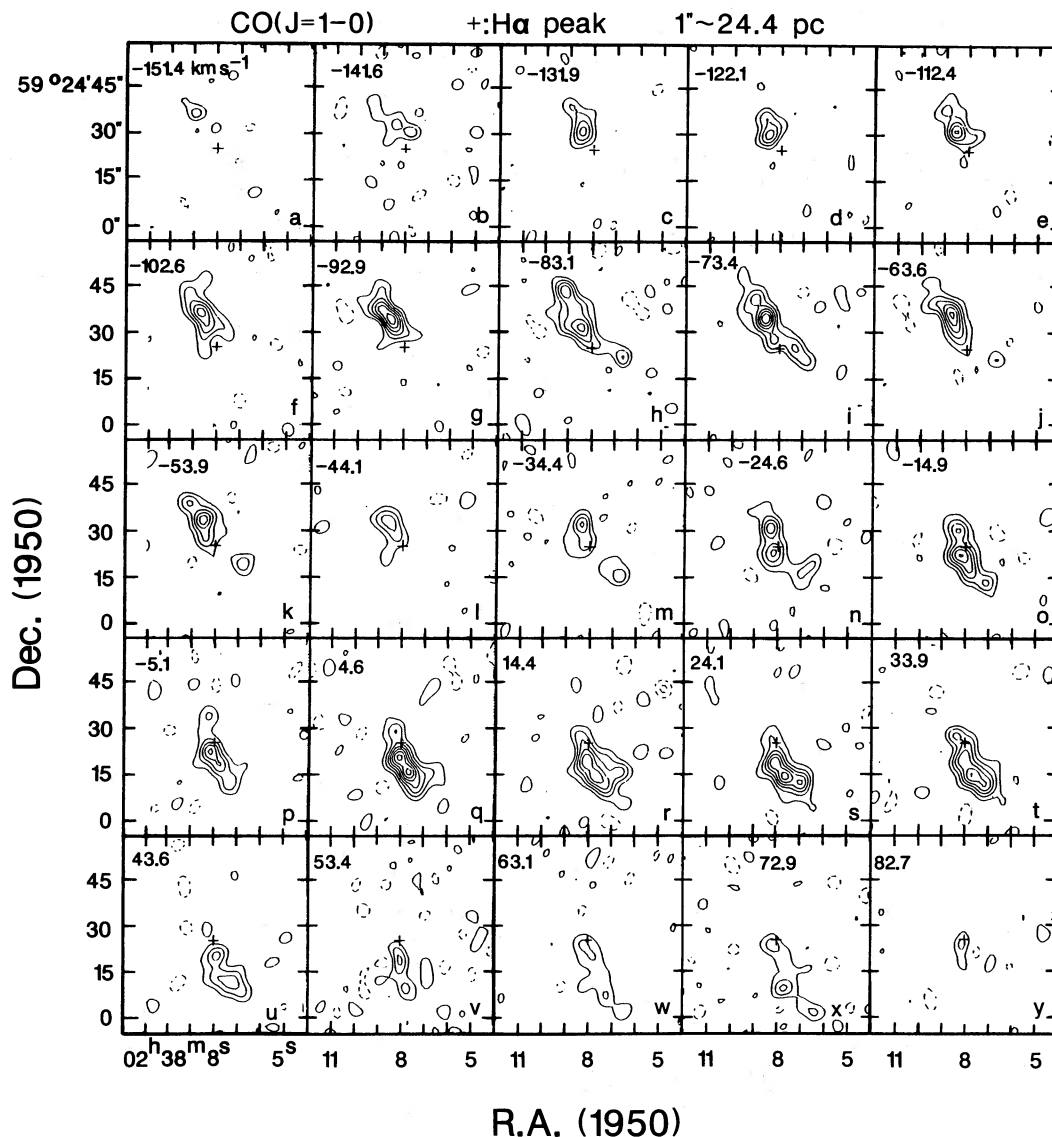


FIG. 2.—CO channel maps for 25 velocity channels with a velocity width of 9.75 km s^{-1} , ranging from $V_{\text{lsr}} = -151.4 \text{ km s}^{-1}$ to 82.7 km s^{-1} . A contour interval of each map is 11 K km s^{-1} (2σ noise level of maps). A cross indicates a position of the nuclear $\text{H}\alpha$ peak.

the north the velocity gradient is parallel to the ridge. South and west of the nucleus, the structure is more complicated.

The nuclear H α peak in Figure 1c is shifted about 2" from the line of the molecular ridge. This shift may be produced by the uncertainty in the absolute position of our CO map ($\sim 1''$) and the H α map. As shown in Figure 1d, radio continuum emission at 8 GHz is located at the northern peak of the CO emission.

Figure 2 shows CO maps for 25 velocity channels with a velocity width of 9.75 km s^{-1} ranging from $V_{\text{lsr}} = -151.4 \text{ km s}^{-1}$ to 82.7 km s^{-1} . Each channel map was made averaging over 12 channels in the "FX" correlator. A contour interval for each map is 11 K km s^{-1} corresponding to the 2σ noise level. The other averaged channels did not show significant CO emission.

Figure 3 shows four position-velocity maps along the four lines (A-A' to D-D' in Fig. 1a) parallel to the major axis of the ridge. In the maps along C-C' and D-D', we can see a structure clearly showing the differential rotation of the molecular gas (bar). The most interesting feature is an "oval" pattern indicating existence of large noncircular motion. The pattern is clearly seen in Figures 3a and 3b; the blueshifted part of the pattern is in Figure 3a, and the redshifted part in Figures 3b and 3c. This pattern is very similar to that of the expanding molecular ring observed toward the center of our Galaxy (see review by Oort 1977).

Hatched regions in Figure 4 were made by selecting CO emission regions ($\geq 4 \sigma$ level) in channel maps which clearly contribute to the oval pattern in Figures 3a and 3b. However, the CO emission regions at the east are spatially overlapped

with the molecular ridge (*broken lines* in Fig. 4) and are excluded in the figure. The hatched regions show a ringlike structure and the best fit ring is shown in Figure 4. The center of the ring is shifted by $\sim 4''$ from the nucleus to SW. The size of the ring is about $20''$ (500 pc) in its major axis (P.A. = 40°) and $12''$ (250 pc) in its minor axis. The axial ratio of the ring is consistent with that of the disk of the galaxy with an inclination angle of 60° – 70° . The ring is, therefore, an almost circular ring in the plane of the galaxy which has circular and non-circular motions. The arc in Figure 1a is a part of the ring.

IV. DISCUSSION

a) Molecular Gas Bar

Our results strongly suggest the existence of a molecular gas bar in the nucleus of Maffei 2. Similar molecular bar structure are observed in the central regions of the nearby spiral galaxies, IC 342 (Lo *et al.* 1984) and NGC 6946 (Ball *et al.* 1985), and these are interpreted as molecular gas with oval motion in a bar potential. The numerical calculations (Roberts, Huntley, and Albada 1979) show that in barred spiral galaxies shock waves are generated at the leading edges in the bar potential and trailing arms are also generated. An example of such a feature was observed in IC 342 (Lo *et al.* 1984).

In the case of Maffei 2, if we assume that arms slightly seen in the infrared photograph by Spinrad *et al.* (1973) are trailing arms, the NW side of the disk inclines to the nearer side. In such an orientation of the disk, the observed molecular bar can be interpreted as molecular gas in the shock waves at the leading edge. The H α emission distribution shown in Figure 1c

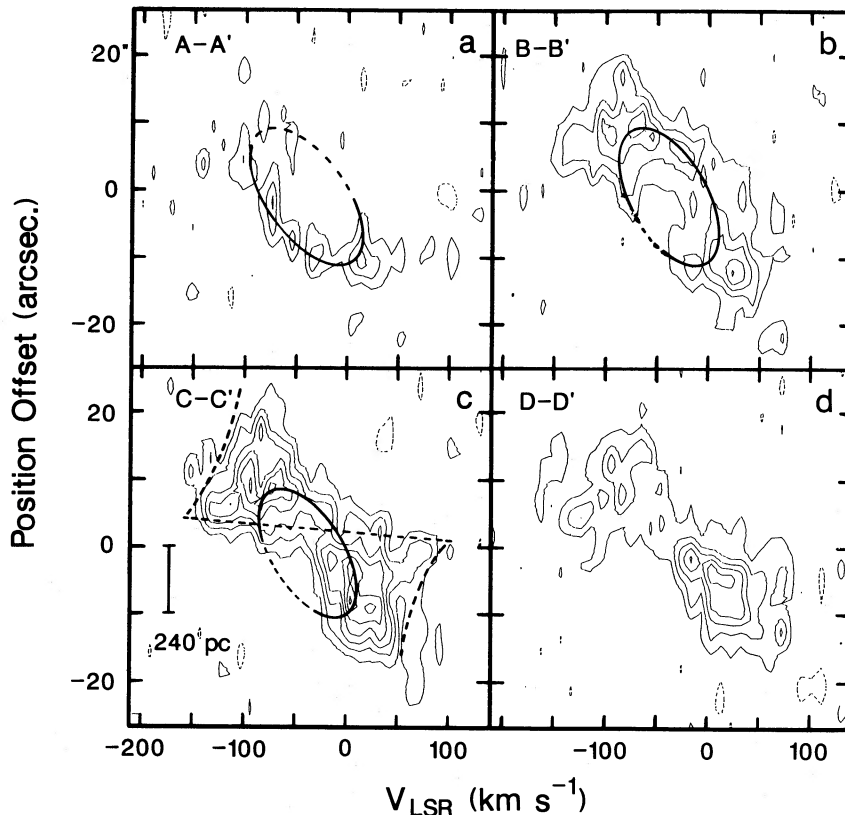


FIG. 3.—Four position-velocity maps along four lines taken parallel to the narrow molecular ridge (bar; P.A. = 25°). The start and end points of each line are shown in Fig. 1a. Position offsets are referred to the nuclear H α peak. Elliptical lines trace oval velocity patterns. A dotted line indicates an adapted rotation curve.

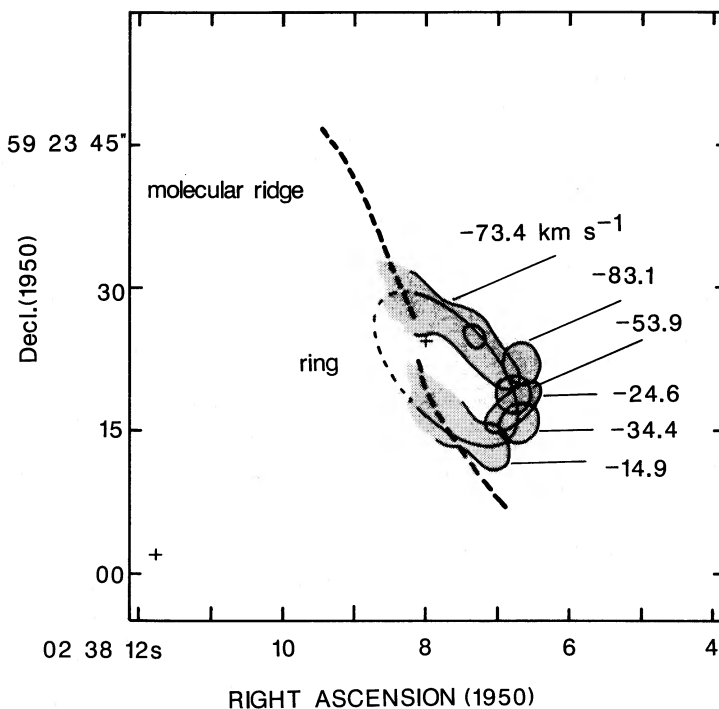


FIG. 4.—Hatched regions indicate selected CO emission regions ($\geq 4\sigma$ level) in the channel maps which clearly contribute to the oval pattern (noncircular motion) in Figs. 3a and 3b. The LSR velocities of selected emission regions are indicated. The CO emission has a ringlike structure. A broken line shows the molecular ridge.

(Spinrad and McCarthy 1988) suggests that the H II regions are also located at the leading side of the northern molecular bar.

Molecular gas in the bar shows not rigid but differential rotation (see Fig. 3). This also suggests that the molecular bar structure may arise in the “traffic jams” of molecular gas at the shock which is formed in the bar potential and is rigidly rotating, if we exclude the possibility that the bar structure is short-lived.

In the molecular bar, noncircular motion due to streaming motion along the bar is expected. Weliachew, Casoli, and Combes (1988) found a misalignment between the elongation of CO emission and the velocity gradient and suggested that this was due to oval distortion of gravitational potential. Figure 1 shows a similar misalignment at the southern part of the molecular bar. The isovelocity contours, however, have complicated structures at the central part and the misalignment is not clear at the northern part. This is probably because of confusion by the large noncircular motion attributed to the ring. This is also because of the orientation of the molecular bar. The bar in Maffei 2 is aligned almost perpendicular to the line of sight because the position angle of the bar, 25° – 30° , is almost the same as that of the major axis of the galaxy obtained from H I observations, 26° – 35° (Shostak and Weliachew 1971; Allen and Raimond 1972; Love 1972; Wright and Seielstad 1973). The streaming motion is, therefore, nearly perpendicular to the line of sight and the line-of-sight velocity of the motion is small. If the axis of the bar is inclined from the major axis of the galaxy by $< \pm 10^\circ$ and gas in the bar has a streaming velocity, $V_s = 100 \text{ km s}^{-1}$, the line-of-sight velocity, $V_s \sin(i) \sin 10^\circ$, is $< \pm 15 \text{ km s}^{-1}$, where i is an inclination angle of the galaxy.

The total mass of molecular gas detected in our observations

was estimated to be $2.4 \times 10^8 M_\odot$. The mass has a range of a factor 2 which is caused by the uncertainty of the CO/H₂ conversion factor and by the uncertainty in total CO flux. In our estimation, we used the standard conversion factor from CO integrated intensities to H₂ column densities (Young and Scoville 1982) corrected for the main beam efficiency (0.6) of the FCRAO 14 m telescope, $4 \times 10^{20} \times 0.6$. We also used a total CO flux of $1460 \text{ Jy km s}^{-1}$ in the CO integrated intensity map (Fig. 1a). The obtained mass is consistent with masses, $2 \times 10^8 M_\odot$ derived by Weliachew *et al.* (1988; $\sim 1'$ area), by Sargent *et al.* (1985; $\sim 30''$ area) within the uncertainties. A mean density of H₂ molecules in the bar, 3 – $11 \times 10^2 \text{ cm}^{-3}$, is obtained assuming a volume, $100 \text{ pc} \times 100 \text{ pc} \times 1000 \text{ pc}$. The thickness of the molecular bar is estimated to be about 100 pc in the plane of galaxy. The thickness of the shocks is, however, probably narrower.

The H α peaks are located at the leading edge of the northern bar with a distance of about 100 pc from the bar. This implies star formation from shocked molecular gas and ensuing ionization by newly formed stars. The time scale for star formation is roughly estimated about 10^{6-7} yr assuming the velocity of the shocked gas relative to the shocks, 100 km s^{-1} . This is consistent with a free fall time of gas with an H₂ density of 10^{2-4} cm^{-3} .

b) Expanding Molecular Ring

The ring shows large noncircular motion (see Figs. 3 and 4). There are three dynamical models for the origin of the noncircular motion. One is the same streaming (elliptical) motion responding to the oval potential (Sørensen, Matsuda, and Fujimoto 1976; Roberts, Huntley, and Albada 1979; Huntley 1980) as that of molecular gas in the bar. The other two are expansion and contraction. There are some arguments against the

model of the streaming motion. (1) The ring seems to be nearly circular in the plane of the disk as mentioned in § III. The location is asymmetric about the nucleus. The circular structure and asymmetry do not match with the streaming motion. (2) Even if the ring has an elliptical structure along the bar, the line-of-sight velocity of the streaming motion is small as discussed in § IVa. The motion cannot explain the large non-circular motion of the ring, 45–50 km s⁻¹. (3) We cannot explain why molecular gas with the streaming motion is in the ring “orbit” in this model.

The noncircular motion can be interpreted as expansion if we assume that the orientation of the disk of the galaxy in § IVa and that the ring is in the plane of the disk, because the NW side of the ring inclines to the nearer side in the orientation and the non-circular velocity at this side is blueshifted (see Fig. 3a). In the expansion model, the ring structure is naturally explained as gas compressed by explosion at the nucleus.

On the other hand, if we assume a special case where the ring is aligned perpendicular to the disk, the noncircular motion is due to contraction to the center. In this model, it is difficult to explain the rotation velocity of the ring indicating that the ring is in the plane of the disk.

It is, therefore, most likely that a ring of molecular gas is expanding in the plane of the galaxy which is also rotating. The expansion and rotation velocities of the ring are estimated to be about 60 km s⁻¹ and 60–70 km s⁻¹, respectively.

The total CO flux of the ring (1030 K km s⁻¹) is estimated from the flux derived for the NW half of the ring, because the SE half of the ring is not distinguished well from the molecular bar in the channel maps. The mass of the ring obtained by the same manner as that of the bar is $6.5 \times 10^7 M_{\odot}$. The kinetic energy of the expansion is 2.4×10^{54} ergs, and a dynamical age is 3×10^6 yr. The kinetic luminosity of the expansion is $3.6 \times 10^6 L_{\odot}$. These parameters of the ring (with uncertainty of a factor 2) are similar to those of the expanding molecular ring observed toward our Galactic center (Kaifu, Kato, and Iguchi 1972; Scoville 1972; Bania 1977; radius = 190 pc, radial velocity = 150 km s⁻¹, and rotation velocity = 60 km s⁻¹, mass $\sim 6 \times 10^7 M_{\odot}$).

c) Origin of Expanding Molecular Ring; Starburst at the Nucleus?

The expanding molecular ring in Maffei 2 is the second example of an outflow of molecular gas in the central disk region of an external galaxy (expansion of a molecular gas ring in NGC 1068 was suggested by Myers and Scoville 1987). The large kinetic energy of expansion and the short dynamical time scale require an “explosive” event in the nucleus. In the starburst nucleus in M82, it is suggested that there exists a vertical outflow of hot ionized gas and molecular gas. The kinetic energy of the molecular outflow is 10^{55-56} ergs and the thermal energy of hot gas is 10^{55} ergs (Watson, Stanger, and Griffiths 1984; Nakai *et al.* 1987). The energies are possibly supplied by supernova explosions. From an analogy with M82, a possible origin of the expanding ring in Maffei 2 is starburst at the nucleus.

There are some arguments supporting the starburst (or

active star formation) in the nucleus of Maffei 2. The far-IR luminosity with a peak at the nucleus, L (40–150 μm) in the central 50" region of Maffei 2 is roughly estimated to be $3 \times 10^9 L_{\odot}$ by Rickard and Harvey (1983). The ratio of the far-IR luminosity to H₂ mass (2.4×10^8), $13 L_{\odot}/M_{\odot}$, is consistent with that in other “starburst” galaxies (typically ~ 10 – $25 L_{\odot}/M_{\odot}$; Sanders *et al.* 1986). Using the far-IR luminosity, we can roughly estimate SFR in the 50" region to be $0.3 M_{\odot} \text{ yr}^{-1}$ from an equation by Scoville and Young (1983). It is probably a lower estimate of SFR at the nucleus, because it is SFR for only massive stars. This means that the H₂ mass was consumed quickly ($< 8 \times 10^8$ yr). Depression (hole) of molecular gas in the central 100 pc region also suggest that the gas may have been consumed by the starburst and the ionization by newly formed stars.

Second, the observed molecular bar suggests the existence of a bar potential. The bar potential plays an important role in an efficient gas supply to the nucleus by the shocks and viscosity, which might lead to the star burst (Lo *et al.* 1984; Ball *et al.* 1985).

Third, there is powerful radio continuum emission (67 mJy at 8 GHz) from the nucleus which is resolved into three point-like sources (see Fig. 1d; Seaquist, Pfund, and Bignell 1976). These sources may be young supernova remnants similar to those observed in M82 (Kronberg, Biermann, and Schwab 1985) and NGC 253 (Antonucci and Ulvestad 1988).

The kinetic energy of the expansion in Maffei 2 can be explained by supernova explosions of a new generation of stars formed from molecular gas in the central 100 pc region (hole). The mass of the gas is estimated to be a few $10^7 M_{\odot}$, assuming that the hole was once filled with molecular gas of the same density as derived for the bar (see § IVa). The duration of the consumption with a SFR of $0.3 M_{\odot} \text{ yr}^{-1}$ would be about 3×10^7 yr. We assume, therefore, that a rate of supernova (SNR) with 10^{51} ergs, about 0.05 yr^{-1} , continued over 10^7 yr. The energy of the expanding ring can be produced with a conversion efficiency of the energy to that of expansion of the ring, ~ 0.01 .

It may be unlikely (Ball *et al.* 1985 in the case of NGC 6946) that the high SFR currently observed in the nucleus could be sustained for the lifetime of the galaxy. Loose, Krugel, and Tutukov (1982) noted that after the birth of a new generation of stars the remaining gas is churned up by supernova explosions, and this terminates the star formation process and leads to an expansion of the gas. It is also likely that a gas sweeping effect by the expanding molecular ring may decrease the gas supply to the nucleus, terminating the starburst activity. The expanding motion of dense gas like the observed ring will be one of the important processes to be considered in studying the duration and repetition of starbursts.

We would like to thank Dr. E. Fomalont for his critical reading of the manuscript and helpful comments. We are indebted to Dr. J. Inatani and Mr. A. Sakamoto for the development of SIS junctions and receivers for the NRO array. We also thank Drs. H. Spinrad and P. J. McCarthy for sending H α images of Maffei 2.

REFERENCES

- Allen, R., and Raimond, E. 1972, *Astr. Ap.*, **19**, 317.
 Antonucci, R. R. J., and Ulvestad, J., S. 1988, *Ap. J. (Letters)*, **330**, L97.
 Ball, R., Sargent, A. I., Scoville, N. Z., Lo, K. Y., and Scott, S. L. 1985, *Ap. J. (Letters)*, **298**, L21.
 Bania, T. M. 1977, *Ap. J.*, **316**, 381.
 Bottinelli, L., Chamaroux, P., Gérard, E., Gouguenheim, L., Heidmann, J., Kazeš, I., and Laugué, R., 1971, *Astr. Ap.*, **12**, 264.
 Chikada, Y., *et al.* 1987, *Proc. IEEE*, Vol. **75**, No. 9, p. 1203.

- Gear, W. K., *et al.*, 1984, *Ap. J.*, **280**, 102.
 Huntley, J. M. 1980, *Ap. J.*, **238**, 524.
 Ishiguro, M., *et al.* 1984, in *Proc. Int. Symp. Millimeter and Submillimeter Wave Radio Astronomy*, Granada, p. 75.
 Ishiguro, M., *et al.* 1989, in preparation.
 Kaifu, N., Kato, T., and Iguchi, T. 1972, *Nature Phys. Sci.*, **238**, 105.
 Kawabe, R., *et al.* 1989, in preparation.
 Kronberg, P. P., Biermann, P., and Schwab, F. R. 1985, *Ap. J.*, **291**, 693.
 Lo, K. Y., *et al.*, 1984, *Ap. J. (Letters)*, **282**, L59.
 Loose, H. H., Krugel, E., and Tutukov, A. 1982, *Astr. Ap.*, **105**, 342.
 Love, R. 1972, *Nature*, **235**, 53.
 Maffei, P. 1968, *Pub. A.S.P.*, **80**, 618.
 Myers, S. T., and Scoville, N. Z. 1987, *Ap. J. (Letters)*, **312**, L39.
 Nakai, N., Hayashi, M., Handa, T., Sofue, Y., Hasegawa, T., and Sasaki, M. 1988, *Pub. Astr. Soc. Japan*, **39**, 685.
 Oort, J. 1977, *Ann. Rev. Astr. Ap.*, **15**, 295.
 Rickard, L. J., and Harvey, P. M. 1983, *Ap. J. (Letters)*, **268**, L7.
 Rickard, L. J., Turner, B. E., and Palmer, P. 1977, *Ap. J. (Letters)*, **218**, L51.
 Roberts, W. W., Huntley, J. M., and Albada, G. D. 1979, *Ap. J.*, **233**, 67.
 Sanders, D. B., Scoville, N. Z., Soifer, B. T., Young, J. S., Schloerb, F. P., Rice, W. L., and Danielson, G. E. 1986, *Ap. J. (Letters)*, **298**, L31.
 Sargent, A. I., Sutton, E. C., Masson, C. R., Lo, K. Y., and Phillips, T. G. 1985, *Ap. J.*, **289**, 150.
 Scoville, N. 1972, *Ap. J. (Letters)*, **175**, L127.
 Scoville, N., and Young, J. 1983, *Ap. J.*, **265**, 148.
 Seaquist, E. R., Pfund, J., and Bignell, R. C. 1976, *Astr. Ap.*, **48**, 413.
 Shostak, G. S., and Weliachew, L. 1971, *Ap. J. (Letters)*, **169**, L71.
 Sørensen, S. A., Matsuda, T., and Fujimoto, M. 1976, *Ap. Space Sci.*, **43**, 491.
 Spinrad, H., Bahcall, J., Becklin, E. E., Gunn, J. E., Kristian, J., Neugebauer, G., Garmir, G., and Dieters, N. H. 1971, *Ap. J. (Letters)*, **163**, L25.
 Spinrad, H., Bahcall, J., Becklin, E. E., Gunn, J. E., Kristian, J., Neugebauer, G., Sargent, W. L. W., and Smith, H. 1973, *Ap. J.*, **180**, 351.
 Spinrad, H., and McCarthy, P. J. 1988, private communication.
 Ulich, B. L. 1981, *A.J.*, **86**, 1691.
 Watson, M. G., Stanger, V., and Griffiths, R. E. 1984, *Ap. J.*, **286**, 144.
 Weliachew, L., Casoli, F., and Combes, F. 1988, *Astr. Ap.*, **199**, 29.
 Wright, M. C. H., and Seilstad, G. A. 1973, *Ap. Letters*, **13**, 1.
 Young, J., and Scoville, N. 1982, *Ap. J.*, **258**, 467.

Y. CHIKADA, M. ISHIGURO, H. IWASHITA, K. HANDA, T. KANZAWA, T. KASUGA, R. KAWABE, H. KOBAYASHI, K.-I. MORITA, N. NAKAI, and T. TAKAHASHI: Nobeyama Radio Observatory, National Astronomical Observatory, Minamimaki, Minamisaku, Nagano, 384-13, Japan

S. ISHIZUKI, Y. MURATA, and S. K. OKUMURA: Department of Astronomy, University of Tokyo, Bunkyo, Tokyo, 113, Japan